Facile Addition and Elimination Reactions of Fluorocarbon Acids at Platinum

A. R. Siedle,* R. A. Newmark, and W. B. Gleason

Contribution from the Science Research Laboratory, 3M Central Research Laboratories, St. Paul, Minnesota 55144. *Received March 15, 1985*

Abstract: Reaction of the fluorocarbon acid $H_2C(SO_2CF_3)_2$ with $(Ph_3P)_2Pt(C_2H_4)$ yields *trans*-$(Ph_3P)_2PtH[C\text{-}HC(SO_2CF_3)_2]$ in which restricted rotation about a covalent Pt–C bond was demonstrated by multinuclear NMR spectroscopy. This compound rearranges to the cis isomer by first-order kinetics and is rapidly solvolyzed by Lewis bases to afford *trans*-$(Ph_3P)_2PtHL^+$-$HC(SO_2CF_3)_2^-$ (L = CH_3CN, DMF, CH_3OH, H_2O, and THF). Complexes containing weak Lewis bases (THF and CH_3OH) are unstable and dimerize to form $(Ph_3P)_3Pt_2(\mu\text{-}H)(\mu\text{-}PPh_2)Ph^+HC(SO_2CF_3)_2^-$ [crystal data: space group $P\bar{1}$, a = 14.039 (2) Å, b = 20.318 (3) Å, c = 13.626 (3) Å, α = 94.43 (1)°, β = 95.69 (1)°, γ = 77.47 (1)°, Z = 2, R = 0.059]. Solvolysis of the cis isomer is slower by a factor of ca. 18.

The organometallic chemistry of fluorocarbon acids of the type $HCR(SO_2R_f)_2$ (R = H, alkyl, and aryl; R_f = perfluoroalkyl) is an area of continuing interest on account of the unusual properties of these materials. Previously, we have outlined their reactions with transition-metal hydrides and found that they behave as strong, nonhygroscopic protic acids whose conjugate bases showed no tendency to coordinate to low-valent metal centers.[1,2] Here reported are oxidative addition reactions of such fluorocarbon acids which lead to the first compounds containing two-center bonds between a metal and the central, methine carbon atom in $RC(SO_2R_f)_2$. These new organometallic compounds display reactivity patterns quite different from conventional metal–alkyl derivatives and thus considerably expand the scope of bis[(perfluoroalkyl)sulfonyl]alkane chemistry.

Results

Addition of 1 equiv of $H_2C(SO_2CF_3)_2$ to $(Ph_3P)_2Pt(C_2H_4)$ in toluene at room temperature produces insoluble *trans*-$(Ph_3P)_2PtH[C\text{-}HC(SO_2CF_3)_2]$, **1**, in 89% yield as a white microcrystalline solid. In CD_2Cl_2 solution at <−30 °C, the $[^1H]^{31}P$ NMR spectrum reveals an AB quartet with δ_A 19.0, δ_B 26.0, J_{AB} = 385, J_{PtPa} = 3060, and J_{PtPb} = 2695 Hz. The inequivalence of the two triphenylphosphine ligands is attributed to an asymmetric orientation of the $C\text{-}HC(SO_2CF_3)_2$ ligand and restricted rotation about the Pt–C bond.[3] Analysis of the reversible ^{31}P NMR spectra over a sufficiently wide temperature range to obtain accurate thermodynamic parameters for the rotational barrier is frustrated by a concomitant isomerization of **1** (vide infra); however, ΔH_{act} at 22 °C, 14.6 kcal mol^{-1}, was determined by total line-shape analysis of the ^{31}P NMR spectrum.[4] This process, with attendant line broadening, obscures additional coupling in the ^1H and ^{19}F NMR spectra, readily apparent at ≤−30 °C (c.f. Table I), between the two nonequivalent ^{31}P nuclei and the methine proton and between ^{195}Pt and ^{19}F in the CF_3 groups. Such coupling, together with the 370 Hz J_{PtC} splitting, establishes that the $HC(SO_2CF_3)_2$ ligand is covalently bonded to platinum through the methine carbon atom and is not present as an anion. The ^1H chemical shift of this fluorocarbon ligand covalently bonded to Pt(II), 4.96 ppm, is ca. 1 ppm to lower field than in compounds containing ionic $HC(SO_2CF_3)_2^-$, 3.9 ppm. This chemical shift difference, together with long-range coupling of the methine proton to ^{31}P and Pt–*H* nuclei, provides a spectroscopic means of recognizing the $C\text{-}HC(SO_2CF_3)_2$ ligand. ^{19}F NMR shifts are different as well: −77 ppm for $C\text{-}HC(SO_2CF_3)_2$ and −81 ppm for anionic $HC(SO_2CF_3)_2^-$.

In CD_2Cl_2 solution, **1** isomerizes to *cis*-$(Ph_3P)_2PtH[C\text{-}HC(SO_2CF_3)_2]$, **2**, whose NMR parameters are given in Table I. As with **1**, spin coupling between the ^1H, ^{13}C, and ^{19}F nuclei in the $C\text{-}HC(SO_2CF_3)_2$ group and ^{195}Pt indicates a covalent bond between the metal and this ligand. The P–P interaction is only 13 Hz, consistent with a cis disposition of these nuclei. The kinetics of the trans-to-cis rearrangement are first-order in concentration of **1**. The rate constant was determined by the procedure of Frost and Pearson[5] in which the approach to equilibrium is considered to be a first-order process with an effective rate constant which is the sum of the constants for the forward and reverse directions. Figure 1 shows a plot of ln $(T_0 - T_e)/(T - T_e)$ vs. time, where T is the concentration of the trans isomer, determined by integration of the ^1H NMR spectrum, at a given time, T_e is the equilibrium concentration of **1**, and T_0 its initial concentration. Linearity of the logarithmic plot is indicative of a first-order process. Least-squares analysis gives the sum of the rate constants as 1.16 × 10^{-4} s^{-1} at 22 °C. The equilibrium constant at this temperature is 2.74 from which the rate constant for trans–cis isomerization is 8.50 × 10^{-5} s^{-1} and the free energy difference between **1** and **2** is 592 cal mol^{-1}. At 40 °C, K_{eq} is 2.52 and k = 8.65 × 10^{-4} s^{-1}. The free energy of activation is essentially temperature invariant, being 22.76 and 22.74 kcal mol^{-1} at 22 and 40 °C, respectively, indicating that ΔS_{act} is nearly zero. The

Table I. Chemical Shifts (ppm) and Coupling Constants (Hz) for $(Ph_3P)_2PtH\{HC(SO_2CF_3)_2\}$[a]

assignment	trans	cis
^1H		
hydride	−12.55	−6.36
	J(H,P) = 10.5, 16.0	J(H,P) = 12.5, 186.5
	J(H,Pt) = 1005	J(H,Pt) = 841
	J(H,H) = 2.1	J(H,H) = 3.1
$HC(SO_2CF_3)_2$	4.96	4.93
	J(H,H) = 1.9	J(H,H) = 3.5
	J(H,P) = 4.8, 6.6	J(H,P) = 7.1, 11.0
	J(H,Pt) = 64	J(H,Pt) = 70
^{19}F	−77.4	−76.0
	J(Pt,F) = 8.0	J(Pt,F) = 18
^{31}P	19.0	18.6
	J(P,P) = 385	J(P,P) = 13
	J(P,Pt) = 3060	J(P,Pt) = 3615
		J(P,H) = 180
	26.0	28.5
	J(P,P) = 385	J(P,P) = 14
	J(P,Pt) = 2965	J(P,Pt) = 2102
		J(P,H) = 13
^{195}Pt		−3830
^{13}C		
$HC(SO_2CF_3)_2$	58.0	63.5
	J(Pt,C) = 370	J(Pt,C) = 500
		J(C,H) = 148

[a] Trans spectra obtained at −38 °C; cis at +22 °C.

(1) Siedle, A. R.; Newmark, R. A.; Pignolet, L. H.; Howells, R. D. *J. Am. Chem. Soc.* **1984**, *106*, 1510.
(2) Siedle, A. R.; Newmark, R. A.; Pignolet, L. H. *Inorg. Chem.*, in press.
(3) Restricted rotation about Pt–C bonds has been observed in, e.g., *trans*-$(PhPMe_2)_2Pt(CH{=}CHPh)_2$ by: Empsall, H. D.; Shaw, B. L. Stringer, A. J. *J. Organometal. Chem.* **1975**, *96*, 461.
(4) Kaplan, J. I. *J. Chem. Phys.* **1952**, *28*, 278.
(5) Frost, A. A.; Pearson, W. G. "Kinetics and Mechanism", 2nd ed.; Wiley: New York, 1961; p 186.

0002-7863/86/1508-0767$01.50/0

Table II. Chemical Shifts (ppm) and Coupling Constants (Hz) for $(Ph_3P)_2PtH(L)^+\{HC(SO_2CF_3)_2\}^-$ [a]

		CD_3CN	$(CD_3)_2NCOD$	THF-d_8	CD_3OD	H_2O
^1H						
hydride		−16.62	−22.70	−24.58	−24.03	−23.09
	J(P,H)	11.9	13.5	13.5	13.6	13.2
	J(H,Pt)	1150	1318	1410	1388	1318
$CH(SO_2CF_3)^-$		3.88	3.91	*b*	*b*	
^{31}P		29.4	33.6	33.4	32.7	31.6
	J(P,Pt)	2901	3026	3019	3030	3006

[a] ^{19}F, −81.0 ppm in CD_3CN salt. [b] Obscured due to overlap with solvent.

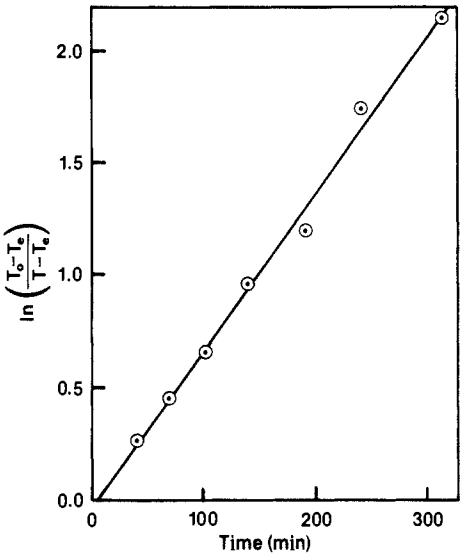

Figure 1. Plot of concentration of **1** vs. time for isomerization of **1** to **2**.

kinetics and product distribution are unaffected by addition of 3 equiv of $PhCH(SO_2CF_3)_2$, indicating that the isomerization does not involve reductive elimination of $H_2C(SO_2CF_3)_2$.

The Pt-C bond in *trans*-$(Ph_3P)_2PtH[C\text{-}HC(SO_2CF_3)_2]$ is readily cleaved in solvolysis reactions with Lewis bases. Dissolution of **1** in acetonitrile, dimethylformamide, methanol, or aqueous tetrahydrofuran results in rapid, quantitative formation of *trans*-$(Ph_3P)_2PtH(L)^+HC(SO_2CF_3)_2^-$ (**3**, L = CH_3CN; **4**, L = DMF; **5**, L = CH_3OH; **6**, L = H_2O). In the latter, mixed solvent, $(Ph_3P)_2PtH(H_2O)^+$ and $(Ph_3P)_2PtH(THF)^+$ are in equilibrium. NMR data for these compounds are given in Table II. The $HC(SO_2CF_3)_2^-$ ion exhibits sharp, singlet ^1H and ^{19}F resonances at 3.9 and −81 ppm, respectively, with no indication of coupling to phosphorus or platinum as was seen in the carbon-bonded compounds **1** and **2**. Solutions of **3** and **4** in their respective ligands are stable at room temperature for at least several days. As indicated below, reaction with tetrahydrofuran is distinctive.

Proton spectra of *trans*-$(Ph_3P)_2PtH[C\text{-}HC(SO_2CF_3)_2]$ in tetrahydrofuran-d_8 over the temperature range −80 to 22 °C reveal that **1** is in equilibrium with its solvolysis product *trans*-$(Ph_3P)_2PtH(THF)^+HC(SO_2CF_3)_2^-$, **7**. The **1**:**7** ratio varies from 3.3 at −80 °C to 1.3 at 22 °C. From the linear relationship of ΔG with temperature, the thermodynamic parameters for the equilibrium solvolysis reaction are found to be ΔH_0 = 2.3 kcal mol^{-1} and ΔS_0 = 7.5 eu.

Tetrahydrofuran solutions of **7** decompose at room temperature in a reaction quantitative by ^{31}P NMR criteria to yield a phosphide-bridged platinum dimer $(Ph_3P)_3Pt_2(\mu\text{-}H)(\mu\text{-}PPh_2)Ph^+HC(SO_2CF_3)^-$, **8**, whose structure has been determined by single-crystal X-ray diffraction methods, c.f. Figure 4. The quite

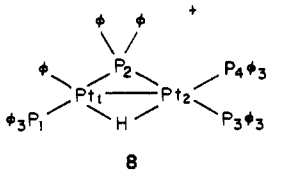

8

complex ^1H, ^{31}P, and ^{195}Pt spectra of this cluster are shown in

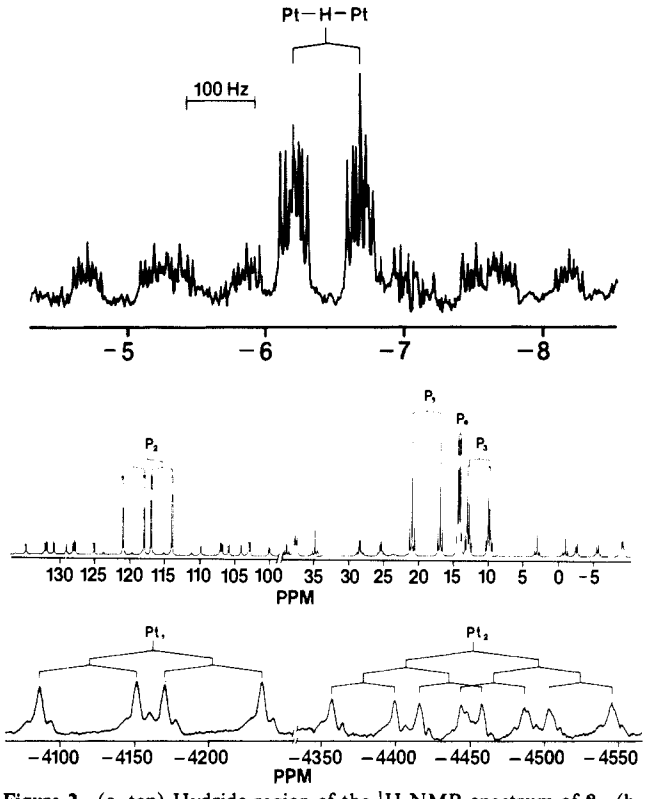

Figure 2. (a, top) Hydride region of the ^1H NMR spectrum of **8**. (b, bottom) ^{31}P (upper trace) and 4.6-T ^{195}Pt NMR (lower trace) spectra of **8**.

Table III. Coupling Constants and Chemical Shifts in Pt Dimers **8** and **8a**

chem shifts, ppm	Ar = Ph	Ar = *p*-FPh	coupling const, Hz	Ar = Ph	Ar = *p*-FPh
δ(H)	−6.46	−6.59	$J(P_1,P_2)$	324.1	334.0
			$J(P_1,P_3)$	<3.0	<6.0
$\delta(P_1)$	18.9	16.3	$J(P_1,P_4)$	<3.0	<6.0
$\delta(P_2)$	117.3	116.8	$J(P_1,Pt_1)$	2898.7	2885.0
$\delta(P_3)$	11.4	9.7	$J(P_1,Pt_2)$	57.1	60.0
$\delta(P_4)$	14.2	12.3	$J(P_1,H)$	7.5	7.1
$\delta(Pt_1)$	−4161		$J(P_2,P_3)$	243.9	248.0
$\delta(Pt_2)$	−4451		$J(P_2,P_4)$	12.4	11.0
			$J(P_2Pt_1)$	2249.6	2224.0
			$J(P_2,Pt_2)$	1800.0	1818.0
			$J(P_2,H)$	11.5	11.9
			$J(P_3,P_4)$	18.0	19.0
			$J(P_3,Pt_1)$	55.8	52.0
			$J(P_3,Pt_2)$	2509.1	2519.0
			$J(P_3,H)$	18.5	18.3
			$J(P_4,Pt_1)$	34.3	44.0
			$J(P_4,Pt_2)$	3786.8	3818.0
			$J(P_4,H)$	96.0	95.0
			$J(H,Pt_1)$	330.0	332.0
			$J(H,Pt_2)$	597.0	595.0
			$J(Pt_1,Pt_2)$	560.0	

Figure 2, and chemical shifts and coupling constants are collected in Table III. These serve to establish, with the exception of the

existence of the phenyl–Pt group, the gross molecular architecture of **8**. The large downfield shift of one of the four ^{31}P resonances is indicative of a diphenylphosphide group bridging two metal atoms,[6] and the phosphorus atom in it, P2, is coupled to, inter alia, two nonequivalent ^{195}Pt nuclei. The ^1H NMR spectrum discloses one hydride resonance at −6.5 ppm with different coupling to all four nonequivalent ^{31}P nuclei. Importantly, two pairs of ^{195}Pt satellites are observed which establishes that this hydride, not observed in the electron density maps, bridges the two platinum atoms. The ^1H noise-decoupled ^{195}Pt NMR spectrum (cf. Figure 2) reveals two Pt resonances. The downfield double–doublet exhibits large coupling to two ^{31}P nuclei, whereas the upfield signal is a doublet of doublets due to splitting from three phoshorus atoms. The undecoupled spectrum indicates, in addition, a 600 Hz coupling on the low field signal, allowing an unambiguous assignment of all the ^{195}Pt coupling constants in Table III. Satellites are observed about each multiplet due to the 560 Hz Pt–Pt coupling, a value sufficiently large to indicate that the two metal atoms are directly bonded.[7] The line widths in the 42.9 MHz (4.6 T) spectra are 190 Hz but only about 100 Hz on spectra obtained at 21.4 MHz from which the more accurate J_{Pt-Pt} data were obtained. The increased line width at higher field is due to chemical shift anisotropy.[8] Additional stereochemical information may also be extracted. For example, P2 is strongly coupled to P3 (244 Hz) and P1 (324 Hz), and the bridging phosphorus atom thus has a trans relationship to these two Ph_3P ligands. Coupling to *cis*-P4 is much smaller, 12 Hz. P3 and P4 may be identified by the small 18 Hz geminal PP coupling, and of these, P4 exhibits a 96 Hz coupling to the *trans*-hydride while the *cis*-P3–H splitting is only 19 Hz. P1 may be recognized by its 324 and 8 Hz J_{P1P2} and (*cis*) J_{P1H} splittings.

The platinum dimer is also formed by the slow decomposition of *trans*-$(Ph_3P)_2PtH(CH_3OH)^+HC(SO_2CF_3)_2^-$, **5**, in methanol, and indeed, **8** is conveniently synthesized simply by recrystallization of **1** from hot methanol, ethanol, or 2-propanol. However, the solubility of **1** in neat methanol is inadequate for kinetic investigations by ^1H NMR for which reason these were carried out on the tetrahydrofuranate **7**.

Conversion of **1** to **8** was followed by ^1H NMR at 22 °C in a 0.1 M solution in THF-d_8 and found to be second order in **1**. The kinetic data may be phenomenologically described in terms of three equilibrium reactions, eq 1–3. Solutions of **1** in tetrahydrofuran immediately (i.e., within sample preparation time) form a mixture of **1** and **7**. The equilibrium between these two compounds is slow on the NMR time scale, because separate absorptions are observed for each species, but fast on the time scale for formation of **8**. The line widths of **1** and **7** are the same, ca. 50 Hz, sufficient to coalesce the triplet due to P–H coupling. Equation 2 represents a reductive elimination of $H_2C(SO_2CF_3)_2$ to form as an intermediate solvated, coordinatively unsaturated $(Ph_3P)_2Pt$. This reacts in turn with additional **7** to form the platinum dimer **8**; however, since **1** and **7** are in rapid equilibrium, the intermediate could be intercepted by one or both of these species. The decrease in concentrations of **1** and tetrahydrofuranate salt **7** and the concomitant increase in the concentration of dimer **8** were measured as a function of time. The correlation

trans-$(Ph_3P)_2PtH[C\text{–}HC(SO_2CF_3)_2]$ (**1**) + THF $\overset{\text{fast}}{\rightleftharpoons}$ $(Ph_3P)_2PtH(THF)^+HC(SO_2CF_3)_2^-$ (**7**) (1)

$(Ph_3P)_2PtH(THF)^+HC(SO_2CF_3)_2^- \overset{\text{fast}}{\rightleftharpoons} (Ph_3P)_2Pt(THF)_n + H_2C(SO_2CF_3)_2$ (2)

$(Ph_3P)_2Pt(THF)_n$ + $(Ph_3P)_2PtH(THF)^+ \overset{\text{slow}}{\rightleftharpoons} (Ph_3P)_3Pt_2(\mu\text{-}H)(\mu\text{-}PPh_2)Ph^+$ (**8**) (3)

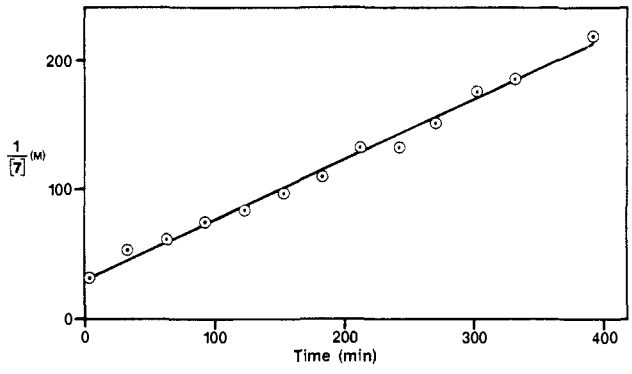

Figure 3. Plot of inverse concentration of **7** vs. time showing second-order kinetics for formation of the phosphide dimer **8**.

coefficient for the linear fit of $[7]^{-1}$ vs. time, c.f., Figure 3, is 0.99. From the slope of this line, the second-order rate constant is 0.007 72 M s^{-1}.

Because the reverse of reaction 2 involves protonation of $(Ph_3P)_2Pt(THF)_n$, the rate of formation of **8** should decrease at longer times due to the increasing concentration of $H_2C(SO_2CF_3)_2$. Solvolysis of an equimolar mixture of **1** and $H_2C(SO_2CF_3)_2$ in THF-d_8 also forms **8** and, for the same reason, the initial rate is 4 times slower in the presence of added acid. However, the effect of $[H_2C(SO_2CF_3)_2]$, either added or arising as shown in eq 2, on the rate of formation of **8** is considerably less than expected. A plausible explanation is that $H_2C(SO_2CF_3)_2$ is not effectively ionized in tetrahydrofuran which has a dielectric constant of only 7.5. In support of this, the molar conductivity of a 0.01 M solution in THF is 7×10^{-2} ohm^{-1} cm^2 mol^{-1} compared with 6 ohm^{-1} cm^2 mol^{-1} for 0.01 M $(n\text{-}C_3H_7)_4N^+HC(SO_2CF_3)_2^-$ in THF. Thus, the kinetic system contains a weak acid and the salt of its conjugate base and effectively comprises a buffer system in which $[H^+]$ is slowly changing. Repetition of the kinetic experiments using ^{31}P NMR as the analytical probe failed to reveal any absorptions attributable to $(Ph_3P)_2Pt(THF)n$, and so its steady-state concentration must be, at most, a few mole percent, the level at which new resonances could be recognized amidst those for reactants and product. However, because added $H_2C(SO_2CF_3)_2$ slows down the rate of formation of **8** and because pure **8** itself does not react with this acid, at least one species intermediate between **7** and **8** is required. In this regard, reactions 1 and 2 are analogous to those developed for other oxidative elimination and addition reactions.[9a,b]

When a 3:1 equilibrium mixture of **1** and **2** is dissolved in tetrahydrofuran, *trans*-$(Ph_3P)_2PtH(THF)^+HC(SO_2CF_3)_2^-$ again forms and is converted to **8** as described above. However, the concentration of **2** decreases approximately 18 times more slowly than that of **1**. Presumably it reacts by slow prior isomerization to the more reactive **1**, a reaction which is considerably faster in dichloromethane.

Formation of the dimer **8** formally involves transfer of a phenyl group from phosphorus (or, alternatively, insertion of platinum into a P–C bond). The regiospecificity of this group transfer was explored with use of *trans*-$[(p\text{-}FPh)_3P]_2PtH[C\text{–}HC(SO_2CF_3)_2]$, **1a**, prepared analogously to **1** but by using tris(*p*-fluorophenylphosphine) instead of Ph_3P. Solvolysis of **1a** in refluxing 2-propanol affords $[(p\text{-}FPh)_3P]_3Pt_2(\mu\text{-}H)[\mu\text{-}(p\text{-}FPh)_2P]\text{-}p\text{-}FPh^+HC(SO_2CF_3)_2^-$, **8a**, whose NMR parameters, shown in Table III, indicate that it has the same chemical structure as **8**. Its ^{19}F NMR spectrum demonstrates doublets (J_{PF} = 2.7 Hz) of triplets (J_{HF} = 5.8 Hz) of triplets (J_{HF} = 8.6 Hz) at −105.60, −105.07, and −106.86 ppm, each integrating for three fluorines and assigned to the three nonequivalent $(p\text{-}FPh)_3P$ ligands. A multiplet at −107.37 ppm (2 F) is assigned to the $(p\text{-}FPh)_2P$ bridge. A multiplet of unit area at −123.50 ppm is observed for the *p*-FPh

(6) Carty, A. J. *Adv. Chem. Ser. No.* **1982**, *196*, 163.
(7) Boag, N.; Browning, J.; Crocker, C.; Goggin, P. L.; Goodfellow, R. J.; Murray, M.; *Spencer*, J. L. *J. Chem. Res Synop.* **1978**, 228.
(8) Dechter, J. J.; Kowalewski, J. J. *J. Magn. Reson.* **1984**, *59*, 146.
(9) (a) Atwood, J. D. "Inorganic and Organometallic Reaction Mechanisms"; Brooks/Cole Publishing: Monterey, CA 1985. (b) Lukehart, C. M. Fundamental Transtion Metal Organometallic Chemistry"; Brooks/Cole Publishing: Monterey, CA 1985.

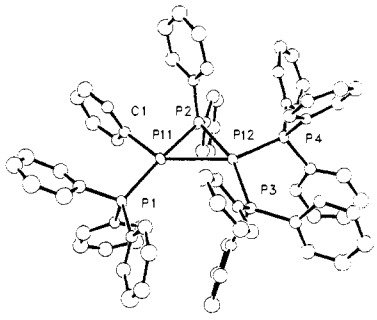

Figure 4. View of the $(Ph_3P)_3Pt_2(\mu\text{-}H)(\mu\text{-}PPh_2)Ph$ cation drawn with 33% probability ellipsoids. Ph_3P ring hydrogens are omitted for clarity.

Table IV. Selected Bond Distances and Angles[a]

	distances, Å		angles, deg
Pt1–Pt2	2.885 (1)	P2–Pt1–Pt2	51.2 (1)
Pt1–P1	2.326 (3)	Pt1–P2–Pt2	79.2 (1)
Pt1–P2	2.239 (3)	P2–Pt2–Pt1	49.7 (1)
Pt1–C1	2.06 (1)	C1–Pt1–P1	91.2 (3)
Pt2–P2	2.289 (3)	C1–Pt1–P2	90.0 (3)
Pt2–P3	2.339 (3)	P1–Pt1–P2	173.4 (1)
Pt2–P4	2.274 (3)	P2–Pt2–P4	99.7 (1)
		P3–Pt2–P4	99.2 (1)
		Pt1–Pt2–P3	111.2 (1)
		P2–Pt2–P3	160.9 (1)

[a] Numbers in parentheses are estimated standard deviations to the least significant digit.

ligand attached to platinum. This resonance is a symmetrical triplet (J_{HF} = 7.5 Hz) of unresolved multiplets. The large triplet splitting indicates that the fluorine is in a ring containing two ortho protons, i.e., that it is para-substituted. The same conclusion can be reached from consideration of the ^{19}F chemical shifts which, in compounds of the type $(m\text{-}FPh)Pt(PEt_3)_2X$ (X = aryl, CH_3, Cl, and Br), are in the range −114.7 to −116.7 ppm but in the *p*-fluorophenylplatinum analogues are in the range −122.7 to −124.9 ppm, as is **8a**.[10,11] Thus, the phenyl-transfer process is regiospecific in that fluorine, originally para to phosphorus in the $(p\text{-}FPh)_3P$ ligands, is also para to platinum in the phosphide-bridged dimer.

Structure of $(Ph_3P)_3Pt_2(\mu\text{-}H)(\mu\text{-}PPh_2)Ph^+HC(SO_2CF_3)_2^-$. Figure 4 shows the important details of the molecular structure of the cation, and selected bond distances and angles are given in Table IV. The Pt_2P unit comprises an unsymmetrical triangle, P1 and the phenyl group being attached to Pt1 and P3 and P4 to Pt2. Within this triangle, the two basal P2–Pt1–Pt2 and P2–Pt2–Pt1 angles, 51.2 (1) and 49.7 (1)°, are considerably more acute than the apical Pt1–P2–Pt angle, 79.2 (1)°. If the phenyl, hydride, and diphenylphosphide ligands are considered to have formal 1− charges, then platinum in **8** is formally in a 2+ oxidation state. Accordingly, the Pt–Pt distance, 2.885 (1) Å, is considerably longer than that in low-valent platinum compounds such as $(Ph_3P)_3Pt_2(CO)S$ [2.647 (2) Å],[12] the clusters $[Pt_3(CO)_3(\mu\text{-}CO)_3]_n^{2-}$ (2.66 Å av.),[13] $(Ph_3P)_2Pt_2(\mu\text{-}PPh_2)_2$ [2.604 (1) Å], and $(Ph_3P)_2Pt_3(\mu\text{-}PPh_2P)_3Pt$ [2.785 (1) Å] but quite comparable to the metal–metal bond lengths of 2.779 and 2.885 Å in *cis*-diammineplatinum α-pyridone blue in which the mean oxidation number of platinum is 2.25+[14] and 2.819 (1) Å in $[(Et_3P)_4Pt_2(\mu\text{-}H)_2Ph]BPh_4$ which, incidentally, has J_{PtPt} = 796 Hz.[15] Because the platinum atoms are spanned by two different bridging ligands, it seems unproductive to attempt to extract the metal–metal bond order from the Pt–Pt distance.

Scheme I

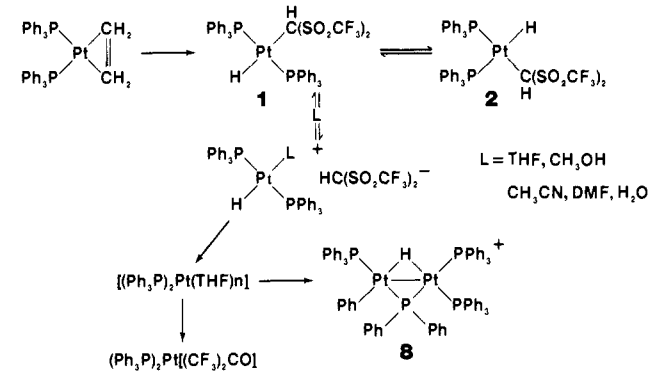

The two phosphide P–Pt contacts are grossly different with *d*(Pt1–P2) and *d*(Pt2–P2) of 2.239 (3) and 2.289 (3) Å, respectively. This is presumably a consequence of the different substitution at the two metal atoms. Curiously, the Pt–P bonds to the external triphenylphosphine ligands, Pt1–P1 and Pt2–P3, are similar, 2.326 (3) and 2.339 (3) Å, respectively, even though the corresponding *trans*-Pt–P distances are not. Of the four Pt–P bonds in the cluster, that between Pt2 and P4, 2.274 (3) Å, is conspicuously short. This is possibly due to a structural trans effect, since the bridging hydride, not located in the structure solution but whose position is quite clear from NMR experiments (vide supra), is trans to P4. Thus, the metrical features of **8** depart from the trend seen in the clusters $(Ph_3)_2Pt_2(\mu\text{-}PPh_2)_2$ and $(Ph_3P)_2Pt_3(\mu\text{-}PPh_2)_3Ph$[16] in which Pt–P phosphide bonds are longer than those between platinum and triphenylphosphine. Phosphorus atoms in the three external triphenylphosphine groups are essentially coplanar with the Pt_2P cluster core: the dihedral angles between the Pt1Pt2P2 plane and those defined by C1Pt1P1 and P4Pt2P3 are 4.7° and 6.5°, respectively, so that the coordination geometry at each platinum atom closely approximates square-planar. Finally, the phenyl ring, whose existence was not apparent from numerous spectroscopic data, is seen to be bonded to Pt1 with *d*(Pt1–Cl) = 2.06 (1) Å, comparable to the 2.07 (1) Å metal–carbon distance in the $(Et_3P)_4Pt_2(\mu\text{-}H)_2Ph^+$ ion.[14] The least-squares plane of this phenyl ring, from which the maximum atomic displacement is 0.03 Å (c.f. supplementary material), is rotated 91.2° with respect to the Pt1Pt2P2 plane.

The distances and angles in the $HC(SO_2CF_3)_2$ anion are very similar to those observed in the rubidium[16] and $(Ph_3P)_4OsH_3^+$ salts.[2]

Discussion

The addition and solvolysis chemistry of $(Ph_3P)_2Pt(C_2H_4)$ and $H_2C(SO_2CF_3)_2$ is summarized in Scheme I. The reaction of these two compounds to form **1** may be viewed as an oxidative addition reaction. In this context, the reactivity of the fluorocarbon acid differs from that of HCl and CF_3SO_3H which are reported to form ethane and $(Ph_3P)_2PtX_2$ (X = Cl and CF_3SO_3)[18] and from FSO_3H which adds to [(4,5-bis[(diphenylphosphino)methyl]-2,2-dimethyl-1,3-dioxolane]$Pt(C_2H_4)$ to form *cis*-$L_2Pt(C_2H_5)(OSO_2F)$.[19] However, the Pt–C σ bond in **1** is quite labile, and this material undergoes solvolysis by even such weak bases as tetrahydrofuran with generation of the $HC(SO_2CF_3)_2^-$ anion. This reactivity is, however, not intrinsic to the Pt–[(C–$HC(SO_2CF_3)_2$] unit since the cis isomer of **1** solvolyzes much more slowly. Pt–C bond cleavage in **1** may therefore be facilitated by the kinetic trans effect of the hydride ligand. The hydride in **1** appears not to be acidic, and no reaction with 1,8-bis[(dimethylamino)naphthalene] (proton sponge) was detectable. Similarly, the platinum hydride in **3** does not exchange with D_2O, but that in **5** exchanges with CD_3OD.

(10) Parshall, G. W. *J. Am. Chem. Soc.* **1964**, *86*, 5637.
(11) Parshall, G. W. *J. Am. Chem. Soc.* **1966**, *88*, 704.
(12) Skapski, A. C.; Troughton, P. G. H. *J. Chem. Soc. A* **1969**, 2772.
(13) Calabrese, J. C.; Dahl, L. F.; Chini, P.; Longoni, G.; Martinengo, S. *J. Am. Chem. Soc.* 1974, *96*, 2614.
(14) Barton, J. K.; Rabinowitz, H. N.; Szalda, D. J.; Lippard, S. J. *J. Am. Chem. Soc.* **1977**, *97*, 2827.
(15) Bachechi, F.; Bracher, G.; Grove, D. M.; Kellenberger, B.; Pregosin, P. S.; Venanzi, L. M.; Zamboneli, L. *Inorg. Chem.* **1983**, *22*, 1031.
(16) Taylor, N. J.; Chieh, P. C.; Carty, A. J. *J. Chem. Soc., Chem. Commun.* **1975**, 448.
(17) Davoy, K. T.; Gramstad, T.; Husebye, S. *Acta Chem. Scand., Ser. A 33A*, **1979**, 359.
(18) Foley, P.; Whiteides, G. M. *Inorg. Chem.* **1980**, *19*, 1402.
(19) Brown, J. M.; Cook, S. J.; Kimber, S. J. *J. Organometal. Chem.* **1984**, *269*, C58.

We consider that subsequent reaction of *trans*-$(Ph_3P)_2PtH(THF)^+$ in tetrahydrofuran involves formation of the reactive intermediate $(Ph_3P)_2Pt(THF)_n$. In this, *n* is experimentally undefined but is likely 1 or 2, corresponding to a 16- or 18-electron configuration, respectively, at the metal. Here, tetrahydrofuran serves to stabilize the putative intermediate $(Ph_3P)_2Pt$ which is reported to disproportionate to $(Ph_3P)_3Pt$ and platinum metal in the absence of additional ligands.[20] The steady-state concentration of this solvate is low, and it is not detectable by ^{31}P NMR. It may, however, be trapped as $(Ph_3P)_2Pt[(CF_3)_2CO]$ when **1** is solvolyzed in tetrahydrofuran containing a large excess of hexafluoroacetone. According to the scheme, dimer **8** results from *formal* condensation of $(Ph_3P)_2Pt(THF)_n$ with **1** or **7** by insertion into Pt–H and P–C bonds. This accounts for the second-order dependence of the rate of formation of **8** on the concentration of **1** and for the observations that on heating in tetrahydrofuran, $(Ph_3P)_2Pt(C_2H_4)$ forms new, yet uncharacterized platinum phosphide compounds but no **8** and that in the dimer synthesized from $PhCD(SO_2CF_3)_2$, deuterium is incorporated into the bridging position. Insertion of coordinately unsaturated Pt(0) complexes into Pt–H bonds is well-established[21] but similar reactions with P–C bonds, which result in transfer of a phenyl group from phosphorus to platinum, remain mechanistically uncharacterized. Prolonged pyrolysis of $(Ph_3P)_3Pt$ in benzene solution generates numerous products among which one, $(Ph_3P)_2Pt_3(\mu\text{-}PPh_2)_3Ph$, contains, as does **8**, both phosphide bridges and a phenyl–Pt group.[15] The condensation reactions involving the fluorocarbon acids, however, are distinctive in that they are selective and proceed in high yields at low temperature. Conceptually, generation of $(Ph_3P)_2Pt(THF)_n$ involves reductive elimination of $H_2C(SO_2CF_3)_2$ from *trans*-$(Ph_3P)_2PtH[C\text{-}HC(SO_2CF_3)_2]$ with the intermediate, *trans*-$(Ph_3P)_2PtH(THF)^+HC(SO_2CF_3)_2^-$, and the product, $(Ph_3P)_2Pt(THF)_n$, being stabilized by coordination with tetrahydrofuran. In contrast to the chemistry of **1** and **2**, where the cis isomer is more stable, in reductive elimination processes not involving nucleophilic solvolysis and in which sequential bond-breaking steps are more nearly contemporaneous, cis isomers are often more reactive. This has been observed in thermolysis of L_2PtRH (L = tertiary phosphine; R = alkyl, aryl) where loss of RH occurs at lower temperatures for the cis than for the trans isomer.[22] Reducive elimination of $RCH(SO_2CF_3)_2$ (R = CH_3 and Ph) is also quite sensitive to steric effects and need not require the assistance of a strong Lewis base. Thus, when $(Ph_3P)_2Pt(C_2H_4)$ in toluene is treated at room temperature with $CH_3CH(SO_2CF_3)_2$ or $PhCH(SO_2CF_3)_2$, $(Ph_3P)_3Pt_2(\mu\text{-}H)(\mu\text{-}PPh_2)Ph^+$ salts are rapidly formed in good yield. These probably arise from *trans*-$(Ph_3P)_2PtH[C\text{-}RC(SO_2CF_3)_2]$ which are too unstable to isolate. **1** exhibits good thermal stability: heating at 100 °C in toluene leads to a mixture containing about equal amounts of **1**, **2**, and **8**. Interestingly, NMR analysis reveals that bis[(trifluoromethyl)sulfonyl]amine, $HN(SO_2CF_3)_2$, forms *trans*-$(Ph_3P)_2PtH(C_2H_4)^+N(SO_2CF_3)_2^-$ which is not a precursor of **8**.

Experimental Section

NMR spectra were recorded on a 4.7-T Varian XL-200 spectrometer for which the ^1H frequency is 200 MHz. Chemical shifts are reported relative to internal $(CH_3)_4Si$ (^1H and ^{13}C) and $CFCl_3$ (^{19}F) or external H_3PO_4 (^{31}P) and aqueous Na_2PtCl_6 (^{195}Pt), positive chemical shifts being downfield of the reference. ^{31}P NMR spectra were obtained with both noise and single-frequency decoupling of the aromatic protons. The 21.4-MHz ^{195}Pt spectra were obtained at 2.3 T on an IBM NR-100 spectrometer. The signal/noise in the ^{195}Pt NMR experiments was insufficient to obtain a spectrum of **1** before extensive isomerization to **2**. Solvents used for NMR experiments, CD_2Cl_2 and THF-d_8, were distilled on a vacuum line from CaH_2 and $LiAlH_4$, respectively. Tetrahydrofuran used for conductance measurements was distilled from sodium benzophenone and stored over clean sodium metal under nitrogen. Toluene was dried using NaK alloy. The fluorocarbon acids were prepared by the method of Koshar and Mitsch.[23]

Table V. Summary of Crystallographic Data

Crystal Parameters	
space group	$P\bar{1}$ (No. 2)
a, Å	14.039 (2)
b, Å	20.318 (3)
c, Å	13.626 (3)
α, deg	94.43 (1)
β, deg	95.69 (1)
ν, deg	77.47 (1)
V, Å^3	3769.1
Z	2
d(calcd), g cm^{-3}	1.59
temp, °C	23
abs coeff, cm^{-1}	39.5
cryst dimensions, mm	0.30 × 0.15 × 0.17
Measurement of Intensity Data	
diffractometer	Enraf-Nonius CAD4
radiation	Mo Kα (λ = 0.71073 Å)
monochromator	graphite crystal
scan type	$\omega - 2\theta$
scan speed (variable), deg min^{-1}	1–20
reflections measured	$\pm h,k,\pm l$
max 2θ, deg	44
no. of reflections	9210 total 8895 unique 5800 with $F_o^2 > 3.0\sigma(F_o^2)$
parameters refined	343
p	0.04
R	0.059
R_w	0.076
esd of unit weight observation	2.45
largest shift/error in final cycle	0.13
largest peak in final diff Fourier, e Å^{-3}	2.85 (near platinum)

***trans*-$(Ph_3P)_2PtH[C\text{-}HC(SO_2CF_3)_2]$, 1.** A solution of 1.8 g (6.3 mmol) of $H_2C(SO_2CF_3)_2$ in 10 mL of toluene was added under nitrogen to a suspension of 4.6 g (6.2 mmol) of $(Ph_3P)_2Pt(C_2H_4)$ in 30 mL of toluene. After stirring overnight, the product was collected on a filter, washed with fresh solvent, and vacuum-dried. The yield of white, powdery **1** was 5.5 g (89%). Anal. Calcd for **1**: C, 46.9; H, 3.2; F, 11.4; P, 6.2; Pt, 19.5; S, 6.4; M_r 999. Found: C, 46.6; H, 3.4; F, 11.0; P, 6.2; Pt, 20.3; S,6.5; M_r (osmometric in $CHCl_3$) 976. The infrared spectrum (Nujol mull) shows a PtH stretching band at 2169 cm^{-1} and absorptions at 1347, 1193, and 1120 cm^{-1} due to the CF_3SO_2 groups: Λ (1 × 10^{-3} M in CH_2Cl_2) 6 Ω^{-1} cm^2 mol^{-1}.

$(Ph_3P)_3Pt_2(\mu\text{-}H)(\mu\text{-}PPh_2)Ph^+HC(SO_2CF_3)_2^-$, 8. 2-Propanol, 50 mL, and 5.5 of **1** were refluxed and stirred under nitrogen for 3 h. The reaction mixture was cooled in a wet ice bath and then filtered to afford 4.5 g (96%) of **8** as a light-yellow powder. Anal. Calcd for **8**: C, 52.4; H, 3.6; F, 6.6; P, 7.2; Pt, 22.7; S, 3.7. Found: C, 52.2; H, 3.4; F, 7.0; P, 7.2; Pt, 21.7; S, 4.0. Attempts to identify a PtH stretching band in the infrared or Raman spectra were unsuccessful: Λ (1.3 × 10^{-3} M in CH_2Cl_2) 39 Ω^{-1} cm^2 mol^{-1}.

Crystallization from hot ethyl acetate yields a 1:1 solvate in which the ethyl acetate, ν_{CO} 1734 cm^{-1}, occupies lattice positions. Subsequent recrystallization of this solvate by rotary evaporation of a dichloromethane–ethanol solution regenerates pure **8**.

Reaction of 0.75 g (1 mmol) of $(Ph_3P)_2Pt(C_2H_4)$ with 0.36 g (1 mmol) of $PhCH(SO_2CF_3)_2$ in 10 mL of toluene produced a light-orange solid. This, after three recrystallizations from dichloromethane–ethanol, afforded 0.41 g (46%) of $(Ph_3P)_3Pt_2(\mu\text{-}H)(\mu\text{-}PPh_2)Ph^+PhC(SO_2CF_3)_2^-$. Anal. Calcd: C, 54.2; H, 3.7. Found: C, 54.5; H, 3.6.

The compound $[(p\text{-}FPh)_3P]_2PtCl_2$ was synthesized from K_2PtCl_4 and $(p\text{-}FPh)_3P$ in refluxing xylene under nitrogen: ^{19}F NMR −107.50 (dtt, J_{PF} = 2.3, $J_{H\text{-}o\text{-}F}$ 5.5, $J_{H\text{-}m\text{-}F}$ = 8.3 Hz); ^{31}P 12.7 (J_{PtP} = 3673 Hz). It was converted to $[(p\text{-}FPh)_3P]_2Pt(C_2H_4)$ (not purified) by the method of Nagel.[24] Reaction with $H_2C(SO_2CF_3)_2$ in toluene provided *trans*-$[(p\text{-}FPh)_3P]_2PtH[C\text{-}HC(SO_2CF_3)_2]$, **1a**: ^1H NMR −12.4 (t, J_{PH} = 14.0, J_{PtH} = 989 Hz), 4.70 ($HC(SO_2CF_3)_2$, J_{PtH} = 61 Hz); ^{19}F NMR −77.4 (s), −108.0, −109.3 (unresolved multiplets); ^{31}P NMR 18.9 (J_{PtP} = 3078 Hz), 25.5 (J_{PtP} = 2982, J_{PP} = 396 Hz). Refluxing **1a** in 2-propanol under nitrogen affords **8a**. In CD_2Cl_2 solution at room temperature, **1a** forms the phosphide-bridged dimer but at a very slow rate and shows no evidence of rearrangement to the cis isomer.

Crystallographic Analysis. Crystals of materials containing the $(Ph_3P)_3Pt_2(\mu\text{-}H)(\mu\text{-}PPh_2)Ph^+$ ion proved quite difficult to obtain. After

(20) Abis, L.; Sen, A.; Halpern, J. *J. Am. Chem. Soc.* **1978**, *100*, 2915.
(21) Paonessa, R. S.; Trogler, W. C. *Inorg. Chem.* **1983**, *22*, 1038.
(22) Arnold, D. P.; Bennett, M. A. *Inorg. Chem.* **1984**, *23*, 2110.
(23) Koshar, R. J.; Mitsch, R. A. *J. Org. Chem.* **1973**, *38*, 3358.
(24) Nagel, U. *Chem. Ber.* **1982**, *115*, 1998.

Table VI. Positional Parameters and Their Estimated Standard Deviations

atom	X	Y	Z	B(A2)	atom	X	Y	Z	B(A2)
Pt1	0.174 08 (4)	0.204 15 (3)	0.331 31 (5)	3.67 (2)	C31	0.416 (1)	0.123 4 (8)	0.369 (1)	4.2 (4)*
Pt2	0.296 80 (5)	0.234 49 (3)	0.190 57 (5)	3.43 (1)	C32	0.486 (1)	0.065 2 (9)	0.371 (1)	5.6 (4)*
P1	0.042 6 (3)	0.277 2 (2)	0.399 3 (3)	3.9 (1)	C33	0.562 (1)	0.060 (1)	0.447 (2)	6.7 (5)*
P2	0.311 8 (3)	0.140 2 (2)	0.277 3 (3)	3.9 (1)	C34	0.566 (2)	0.109 (1)	0.512 (2)	7.1 (5)*
P3	0.239 1 (3)	0.343 6 (2)	0.136 4 (3)	3.9 (1)	C35	0.506 (2)	0.166 (1)	0.511 (2)	8.8 (6)*
P4	0.437 3 (3)	0.205 6 (2)	0.112 9 (3)	3.9 (1)	C36	0.425 (1)	0.175 (1)	0.442 (1)	6.2 (5)*
C1	0.164 (1)	0.129 2 (8)	0.421 (1)	4.4 (4)*	C37	0.308 (1)	0.387 3 (9)	0.064 (1)	4.6 (4)*
C2	0.206 (1)	0.129 0 (9)	0.516 (1)	5.0 (4)*	C38	0.324 (1)	0.363 4 (9)	−0.033 (1)	4.8 (4)*
C3	0.196 (2)	0.078 (1)	0.577 (2)	7.0 (5)*	C39	0.366 (1)	0.399 (1)	−0.092 (2)	6.6 (5)*
C4	0.149 (2)	0.030 (1)	0.542 (2)	7.5 (6)*	C40	0.397 (2)	0.456 (1)	−0.055 (2)	8.3 (6)*
C5	0.109 (2)	0.029 (1)	0.446 (2)	7.9 (6)*	C41	0.380 (2)	0.478 (1)	0.037 (2)	8.1 (6)*
C6	0.112 (1)	0.080 9 (9)	0.384 (1)	4.9 (4)*	C42	0.337 (1)	0.444 (1)	0.099 (1)	6.1 (5)*
C7	−0.060 (1)	0.240 4 (9)	0.419 (1)	4.9 (4)*	C43	0.216 (1)	0.401 6 (8)	0.243 (1)	4.2 (4)*
C8	−0.156 (2)	0.264 (1)	0.369 (2)	8.6 (6)*	C44	0.140 (1)	0.461 (1)	0.241 (2)	6.4 (5)*
C9	−0.234 (2)	0.233 (1)	0.385 (2)	10.1 (7)*	C45	0.137 (2)	0.510 (1)	0.319 (2)	8.0 (6)*
C10	−0.221 (2)	0.186 (1)	0.444 (2)	8.5 (6)*	C46	0.198 (2)	0.501 (1)	0.395 (2)	8.6 (6)*
C11	−0.131 (2)	0.162 (1)	0.500 (2)	8.4 (6)*	C47	0.273 (2)	0.440 (1)	0.404 (2)	7.3 (6)*
C12	−0.050 (2)	0.194 (1)	0.486 (2)	7.4 (6)*	C48	0.277 (1)	0.392 (1)	0.326 (1)	5.9 (5)*
C13	−0.017 (1)	0.357 5 (8)	0.343 (1)	4.2 (4)*	C49	0.127 (1)	0.348 8 (8)	0.056 (1)	4.0 (4)*
C14	−0.043 (1)	0.353 (1)	0.243 (1)	6.1 (5)*	C50	0.092 (1)	0.407 (1)	0.003 (1)	5.9 (5)*
C15	−0.099 (2)	0.408 (1)	0.200 (2)	0.0 (6)*	C51	0.003 (1)	0.408 (1)	−0.059 (2)	6.7 (5)*
C16	−0.124 (2)	0.470 (1)	0.253 (2)	8.4 (6)*	C52	−0.042 (2)	0.358 (1)	−0.068 (2)	7.4 (6)*
C17	−0.093 (2)	0.477 (1)	0.354 (2)	9.0 (7)*	C53	−0.007 (2)	0.301 (1)	−0.020 (2)	7.1 (5)*
C18	−0.043 (1)	0.416 (1)	0.399 (2)	6.4 (5)*	C54	0.080 (1)	0.297 8 (9)	0.044 (1)	5.5 (4)*
C19	0.087 (1)	0.304 0 (8)	0.523 (1)	4.2 (4)*	C55	0.529 (1)	0.129 0 (8)	0.145 (1)	3.8 (3)*
C20	0.182 (1)	0.316 (1)	0.538 (1)	6.1 (5)*	C56	0.513 (1)	0.067 6 (9)	0.112 (1)	4.8 (4)*
C21	0.221 (2)	0.333 (1)	0.637 (2)	7.8 (6)*	C57	0.581 (1)	0.009 (1)	0.132 (1)	5.8 (5)*
C22	0.165 (2)	0.335 (1)	0.710 (2)	7.3 (5)*	C58	0.666 (1)	0.015 (1)	0.188 (2)	6.7 (5)*
C23	0.077 (2)	0.326 (1)	0.697 (2)	8.0 (6)*	C59	0.686 (1)	0.076 (1)	0.218 (2)	6.3 (5)*
C24	0.035 (2)	0.311 (1)	0.604 (2)	7.0 (5)*	C60	0.613 (1)	0.133 (1)	0.201 (1)	6.1 (5)*
C25	0.298 (1)	0.060 5 (8)	0.523 (1)	4.2 (4)*	C61	0.507 (1)	0.271 3 (9)	0.137 (1)	4.5 (4)*
C20	0.182 (1)	0.316 (1)	0.538 (1)	6.1 (5)*	C62	0.488 (1)	0.699 8 (9)	0.768 (1)	5.0 (4)*
C21	0.221 (2)	0.333 (1)	0.637 (2)	7.8 (6)*	C63	0.435 (2)	0.648 (1)	0.741 (2)	7.0 (5)*
C22	0.165 (2)	0.335 (1)	0.710 (2)	7.3 (5)*	C64	0.391 (2)	0.632 (1)	0.810 (2)	8.3 (6)*
C23	0.077 (2)	0.326 (1)	0.697 (2)	8.0 (6)*	C65	0.396 (2)	0.651 (1)	0.903 (2)	8.2 (6)*
C24	0.035 (2)	0.311 (1)	0.604 (2)	7.0 (5)*	C66	0.447 (2)	0.702 (1)	0.929 (2)	7.0 (5)*
C25	0.298 (1)	0.060 5 (8)	0.213 (1)	3.9 (3)*	C67	0.413 (1)	0.192 3 (8)	−0.018 (1)	3.8 (3)*
C26	0.269 (1)	0.057 1 (9)	0.113 (1)	5.3 (4)*	C68	0.489 (1)	0.174 (1)	0.919 (1)	6.0 (5)*
C27	0.252 (1)	−0.003 (1)	0.070 (2)	6.9 (5)*	C69	0.466 (1)	0.164 (1)	0.816 (2)	6.8 (5)*
C28	0.260 (2)	−0.050 (1)	0.118 (2)	7.2 (5)*	C70	0.372 (1)	0.171 (1)	0.780 (2)	6.5 (5)*
C29	0.282 (2)	−0.052 (1)	0.216 (2)	7.9 (6)*	C71	0.298 (1)	0.182 1 (9)	0.836 (1)	5.0 (4)*
C30	0.301 (1)	0.005 (1)	0.268 (2)	6.3 (5)*	C72	0.319 (1)	0.193 6 (9)	0.939 (1)	4.8 (4)*

[a] Starred atoms were refined isotropically. Anisotropically refined atoms are given in the form of the isotropic equivalent thermal parameter defined as $^4/_3[a^2B(1,1) + b^2B(2,2) + c^2B(3,3) + ab\cos\gamma B(1,2) + ac\cos\beta B(1,3) + bc\cos\alpha B(2,3)]$.

30 experiments employing various pure and mixed solvents, light-yellow needles of the 1:1 ethyl acetate solvate, suitable for X-ray structure determination, were obtained by slow diffusion of ethyl acetate into a dichloromethane solution of **8**. A suitable crystal of $(Ph_3P)_3Pt_2(\mu\text{-H})(\mu\text{-PPh}_2)Ph^+HC(SO_2CF_3)_2^-$·ethyl acetate was secured to a glass fiber and found to be triclinic by the Enraf-Nonius CAD4 SDP peak search, centering and indexing programs, and a Delauney reduction calculation.[25] Unit cell measurements were made and refined for 25 reflections in the range $10 < \theta < 15°$. The data collection was begun, and a summary of the crystal and intensity measurement parameters is given in Table V. Background counts were measured at both ends of the scan range with use of an $\omega - 2\theta$ scan, equal at each side to one-fourth of the scan range of the peak. As a check on crystal stability, three check reflections were monitored, and these showed significant decay (28%). Therefore, a linear decay correction was applied.

Lorentz and polarization corrections were applied.[25] An empirical absorption correction based on a series of ψ scans was applied to the data.[26] Relative transmission coefficients ranged from 0.939 to 0.999 with an average value of 0.975.

The structure was solved by using the Patterson heavy-atom method which revealed the positions of the platinum atoms. The remaining non-hydrogen atoms in the cation were located in succeeding difference Fourier syntheses. Positions of phenyl hydrogens were calculated and added to the structure factor calculations, but their positions were not refined. Although all non-hydrogen atoms of the $HC(SO_2CF_3)_2$ anion could be readily located in difference maps, attempts to refine the anion led to unreasonable positional and thermal parameters for both CF_3 groups and one of the four oxygen atoms. Simple disorder models did not correct the problem. Finally, the anion atomic positions were fixed and added to the structure factor calculations but not included in the final refinement. The anion parameters used led to a model in fair agreement with literature data[17] (see supplementary material). A molecule of ethyl acetate was also located in the difference maps and included in the structure factor calculations but not refined. Positional parameters were chemically reasonable and are included in the supplementary data. The final difference Fourier map contained four high peaks (2.8–1.2 e/Å^3) in the vicinity of the platinum atoms (0.9–1.1 Å). The values of the atomic scattering factors were taken from the usual tabulation and the effects of anomalous dispersion were included.[27] The R factors for the final refinement were $R = 0.059$ and $R_w = 0.076$.[28] A list of positional parameters and their estimated standard deviations for non-hydrogen atoms in the $(Ph_3P)_3Pt_2(\mu\text{-H})(\mu\text{-PPh}_2)Ph^+$ cation is given in Table VI. The complete numbering scheme used and additional crystallographic details are found in the supplementary material.

Acknowledgment. We are grateful to Drs. K. A. Brown-Wensley and S. D. Boyd, 3M Science Research Laboratory, for

(25) The intensity data were processed as described in: "CAD4 and SDP Users Manual"; Enraf-Nonius: Delft, Holland, 1978. The net intensity $I = (K/\text{NPI})(C - 2B)$, where $K = 20.1666$(attenuator factor), NPI = ratio of fastest possible scan rate to scan rate for the measurement, C = total count, and B = total background count. The standard deviation in net intensity is given by $(I) = (K/\text{NPI})^2[C + 4B + (pI)^2]$ where p is a factor used to downweight intense reflections.

(26) North, A. C. T.; Phillips, D. C.; Mathews, F. S. *Acta Crystallogr., Sect. A* **1968**, *A24*, 351.

(27) "International Tables for X-ray Crystallography"; Kynoch Press: Birmingham, England, 1984; Vol. IV, Tables 2.2A, 2.2C, and 2.3.1.

(28) The function minimized is $\sum w(|F_o| - |F_c|)^2$ where $w = 1/\sigma^2(F_o)$. The weighted and unweighted residuals are defined as $R = (\sum||F_o| - |F_c||)/\sum|F_o|$ and $R_w = [(\sum w(|F_o| - |F_c|)^2/(\sum w|F_o|)^2]^{1/2}$.

helpful discussions, to J. R. Hill, 3M Analytical and Properties Research Laboratory, for obtaining many of the NMR spectra; to T. Kestner for the 2.3-T ^{195}Pt spectra, and to R. J. Koshar, 3M Industrial and Consumer Sector Laboratory, for gifts of the fluorocarbon acids. Our understanding of the kinetics of platinum dimer formation was facilitated by Dr. G. V. D. Tiers and the helpful comments of a referee.

Supplementary Material Available: Tables of positional and thermal parameters, hydrogen positional parameters, anion and solvent bond lengths, general temperature factor expressions, root-mean-square amplitudes of thermal vibrations, cation bond lengths and angles, torsional angles, least-squares planes, and observed and calculated structure factors (53 pages). Ordering information is given on any current masthead page.

Infrared Photochemistry of Oxetanes: Mechanism of Chemiluminescence

William E. Farneth*[†] and Douglas G. Johnson[‡]

Contribution from the Department of Chemistry, University of Minnesota, Minneapolis, Minnesota 55455, E. I. du Pont de Nemours and Company, Central Research and Development Department, Experimental Station 356/231, Wilmington, Delaware 19898, and Department of Chemistry, University of Chicago, Chicago, Illinois 60637. *Received May 8, 1985*

Abstract: The infrared multiphoton (IRMP) induced photolysis of several oxetanes is examined at low pressures (ca. 100 mtorr) while experimental variables such as laser frequency, laser energy, bath gas, and bath gas pressure are altered. The products of the IRMP induced photolysis of 2-acyl-3-ethoxy-2-methyloxetane, Ox1, are primarily biacetyl and ethyl vinyl ether. When the photolysis is run with the collimated beam of a CO_2 laser (1-3 J/cm^2) luminescence is observed. The intensity of the luminescence varies with the efficiency of the unimolecular decomposition of the oxetane. On the basis of the spectral distribution and temporal behavior of the luminescence following irradiation of Ox1, the emitter is believed to be vibrationally hot electronically excited biacetyl. Similar experiments with 2,2-dimethyl-3-ethoxyoxetane give a weaker emission apparently due to excited-state acetone. Results are discussed in terms of the reverse of the Paterno-Buchi reaction—a diabatic retrophotocycloaddition.

Conventional photochemistry involves a surface crossing at some point along the reaction coordinate. The location of the surface crossing relative to the amount of nuclear reorganization that has occurred has been used to categorize photochemical reactions as "adiabatic" or "diabatic"[1]. Those photochemical reactions where the surface crossing is either the first event following photoexcitation ("hot ground-state reactions") or the last event following all changes in bonding ("chemiluminescent reactions") are termed adiabatic since nuclear reorganization takes place completely on one surface. Those photochemical transformations which return to the ground electronic surface somewhere along the reaction coordinate are referred to as diabatic. Most photochemical reactions are believed to be diabatic.

Infrared multiphoton induced photochemistry is different. Most IRMP induced reactions are adiabatic. Excitation and reaction are usually confined to the ground electronic surface. IRMP induced chemiluminescent reactions are the exception. A number of chemiluminescent processes have been reported. However, these require high laser powers and most involve extensive fragmentation of the reactants to open-shell species.[2-5] One example which appears to give closed-shell species is the IRMP induced decomposition of tetramethyldioxetane (TMD) to yield excited-state acetone.[2] In this case the IRMP induced diabatic chemistry mimics the known thermal chemistry since chemiluminescence in the pyrolysis of TMD is a well-established phenomenon.[6]

We thought it should be possible to extend the observation of IRMP induced chemiluminescence to systems where chemiluminescence had not been observed following thermal excitation. We were particularly interested in systems where the ground-state-to-excited-state surface crossing required for IRMP induced chemiluminescence would constitute the reverse of the excited-state-to-ground-state crossing in a known diabatic conventional photochemical reaction. The photoaddition of ketones and olefins to form oxetanes appeared to be an attractive system for study.[7,8] We have chosen to concentrate on 2-methyl-2-acyl-substituted oxetanes since biacetyl (lowest excited state of about 57 kcal/mol[9]) would be an expected carbonyl fragment in the decomposition. These oxetanes can be made by the addition of photoexcited biacetyl to vinyl ethers.[10] Thus, an IRMP induced diabatic retro-2 + 2-photocycloaddition (evidenced by photon emission from the product) would be the formal reverse of a known diabatic 2 + 2-photocycloaddition.

The IRMP induced photochemistry of three oxetanes, 2-acyl-3-ethoxy-2-methyloxetane (Ox1), 2,2-dimethyl-3-ethoxyoxetane (Ox2), and 2-acyl-2,3-dimethyl-3-methoxyoxetane (Ox3), was studied in some detail. In each case the major products were determined, and the rates (overall) of oxetane loss during pulsed irradiation were measured under various conditions. Ox1 was the most thoroughly examined system. Luminescence has been observed.

Experimental Section

The excitation source used was a pulsed (0.5 Hz), grating turned CO_2 (TEA) laser. The pulse shape, under typical experimental conditions, consisted of an initial spike (250 ns FWHM) followed by a tail out to 1.2 μs. The initial spike delivered 90% of the total pulse energy.

[†] E. I. du Pont de Nemours and Company.
[‡] University of Chicago.

(1) (a) Forster, Th. *Pure Appl. Chem.* **1973**, *34*, 225. (b) Michl, J. *Pure Appl. Chem.* **1975**, *41*, 507.
(2) Yahav, G.; Haas, Y. *Chem. Phys.* **1978**, *35*, 41-49.
(3) Farneth, W. E.; Flynn, G.; Slater, R.; Turro, N. J. *J. Am. Chem. Soc.* **1976**, *98*, 7877.
(4) Watson, T. A.; Mangir, M.; Wittig, C. *J. Chem. Phys.* **1981**, *75*, 5311-5317.
(5) Ambartzumian, R. V.; Chekalin, N. V.; Letokhov, V. S.; Ryabov, E. A. *Chem. Phys. Lett.* **1975**, 36, 301.
(6) Turro, N. J.; Lechtken, P.; Schore, N. E.; Schuster, G.; Steinmetzer, H. C.; Yekta, A. *Acc. Chem. Res.* **1974**, *7*, 97.
(7) Johnson, D. G. Ph.D. Thesis, University of Minnesota, 1985.
(8) Farneth, W. E.; Johnson, D. G. *J. Am. Chem. Soc.* **1984**, *106*, 1875.
(9) Turro, N. J. "Modern Molecular Photochemistry"; Benjamin/Cummings: London, 1978, p 116.
(10) Jones, G., II; Santhanam, M.; Chiang, S. *J. Am. Chem. Soc.* **1980**, *102*, 6077.

0002-7863/86/1508-0773$01.50/0